

VI. RADIO ASTRONOMY*

Prof. A. H. Barrett	A. T. Anderson III	B. R. Kusse
Prof. J. W. Graham	J. C. Blinn III	D. H. Staelin
Prof. R. P. Rafuse	R. K. Breon	D. H. Steinbrecher
Prof. G. Fiocco	J. W. Kuiper	B. K. Yap

A. MILLIMETER RADIO TELESCOPE

1. Status of Research

We have previously described briefly the millimeter radio telescope that is under construction on the roof of the Karl Taylor Compton Laboratories Building.¹ The antenna control facilities are now nearly complete. All elements of the control system have been tested as a complete unit and initial results indicate satisfactory performance. Accurate alignment of the antenna coordinates with the local geodetic coordinate system remains to be accomplished.

We shall undertake in this report to describe in some detail the antenna pointing problem, some of the constraints imposed by the NIKE-AJAX antenna mount and servo system, and details of our solution to an interesting engineering problem.

To set the stage for the following discussion, we review the basic electrical properties of the telescope antenna and its four-millimeter radiometer. A weather-proof version of the radiometer is close to final construction. At 4 mm, the 10-ft parabolic reflector produces a beamwidth of $\sim 0.1^\circ$. The gain of the antenna will be approximately 63 db. Considerable effort has been made to point the antenna beam with an absolute accuracy of 0.01° . It is certain that we can control the pointing incrementally to $\pm 0.01^\circ$, but it is likely that various errors in calibration, computation, and stability may limit absolute pointing accuracy to $\pm 0.02^\circ - 0.03^\circ$. The 4-mm radiometer is now expected to have an rms temperature sensitivity of 1.5°K with an equivalent integration time of 1 second.² Data output from the antenna coordinate encoders and radiometers will be digitally encoded and stored on punched tape. Portions of the experimental use of the system will be automatically programmed. A photograph of the control system equipment located immediately below the antenna is shown in Fig. VI-1.

*This work is supported in part by the National Aeronautics and Space Administration (Grants No. NsG-250-62 and No. NsG-419); in part by the U.S. Navy (Office of Naval Research) under Contract Nonr-3963(02)-Task 2; and in part by Purchase Order DDL BB-107 with Lincoln Laboratory, a center for research operated by Massachusetts Institute of Technology with the joint support of the U.S. Army, Navy, and Air Force under Air Force Contract AF19(604)-7400.

(VI. RADIO ASTRONOMY)

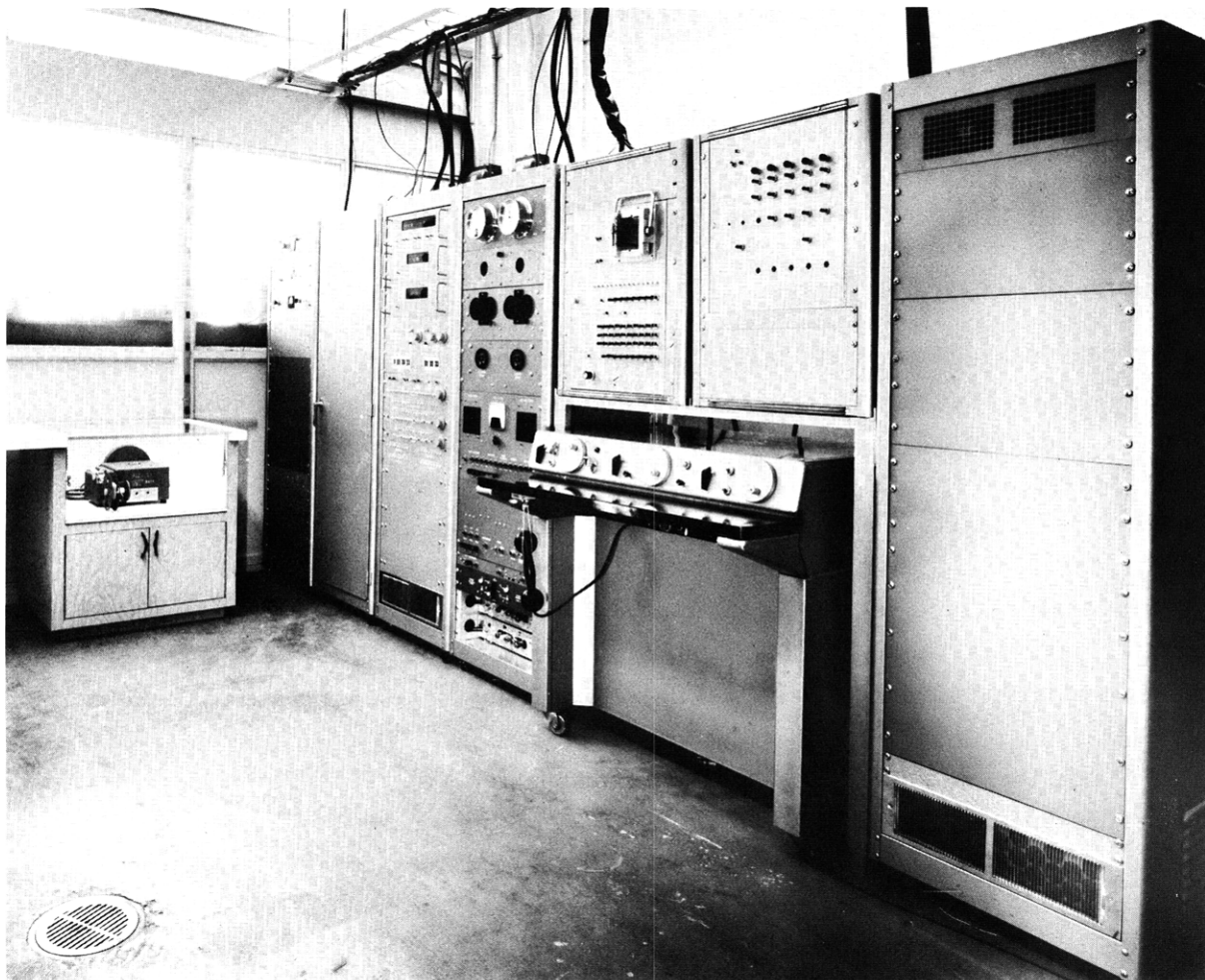


Fig. VI-1. Millimeter radio telescope control facilities.

2. Coordinates and Coordinate Conversion

We shall now review briefly the celestial coordinate system, sidereal time intervals, and the relationship of these quantities to the pointing of an antenna that is steered in conventional azimuth and elevation coordinates. The coordinates of celestial objects of interest to us are found in The American Ephemeris and Nautical Almanac (issued yearly by the Nautical Almanac Office of the United States Naval Observatory). The Ephemeris lists right ascension γ and declination δ at various times. The celestial sphere showing the celestial coordinates γ and δ of an object is shown in Fig. VI-2. Our problem is to determine appropriate azimuth and elevation angles so that the antenna will point to γ and δ . The telescope is situated at N. Lat. $42^{\circ} 21' 37.6''$ and W. Lon. $71^{\circ} 05' 29.7''$. Its rotating platform is, of course, the Earth. Definitions of various sidereal time intervals and angles for relating the telescope position on rotating earth to the celestial

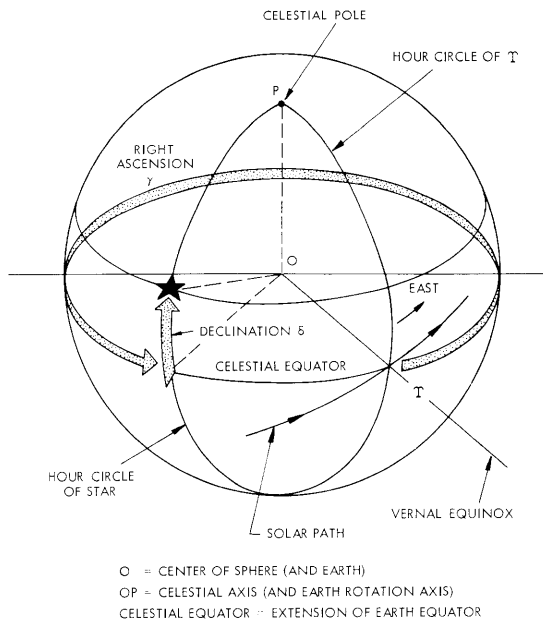


Fig. VI-2. Celestial sphere.

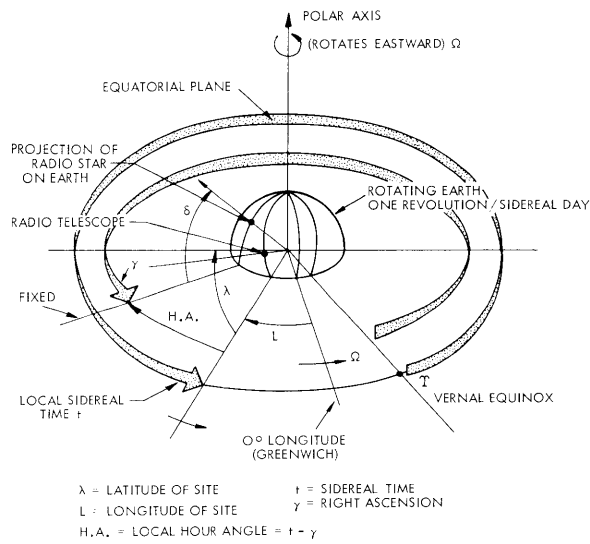


Fig. VI-3. Sidereal time and other angles required for relating radio telescope site on earth to the celestial sphere.

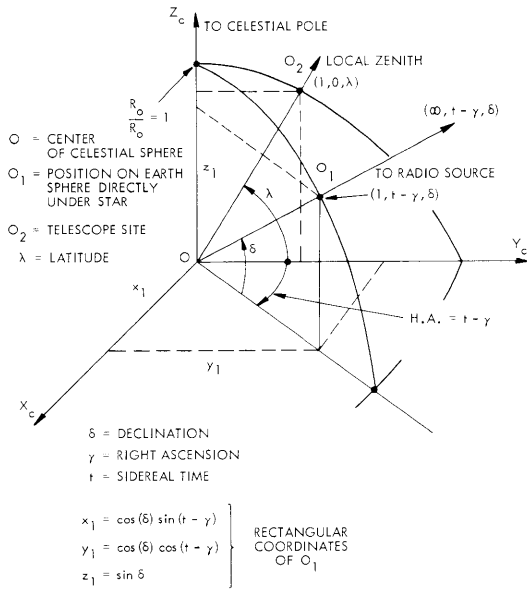


Fig. VI-4. Coordinate transformation: Step I – Polar coordinates (δ, γ) to rectangular coordinates (x_1, y_1, z_1) in the celestial sphere with the rotation of the earth taken into account.

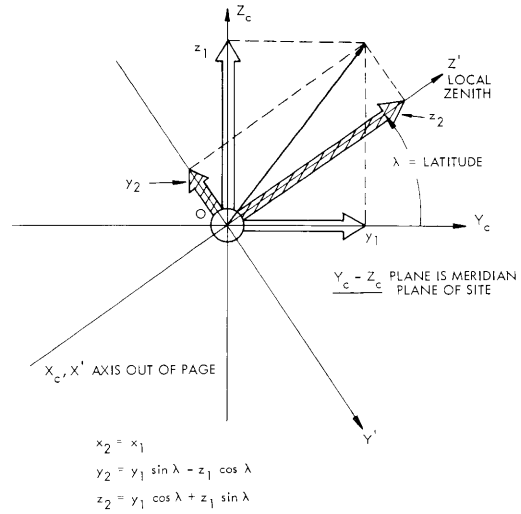


Fig. VI-5. Coordinate transformation: Step II – Rotate about X_c axis to make Z' axis correspond to local zenith.

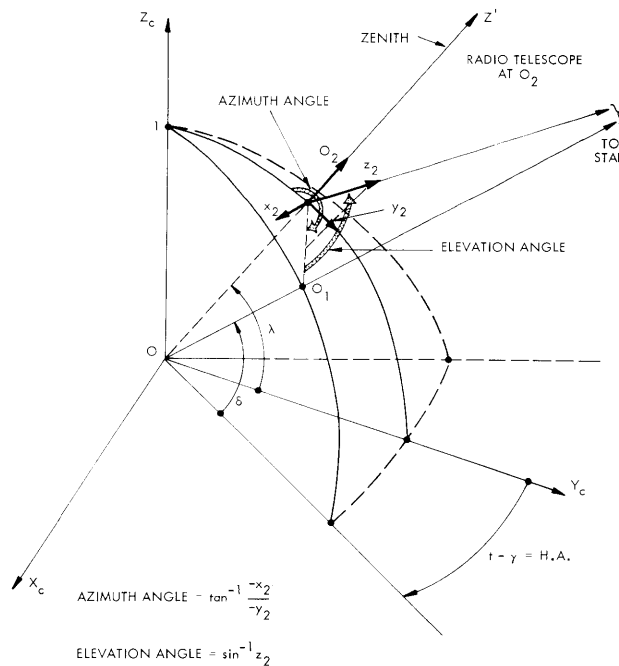


Fig. VI-6. Coordinate transformation: Step III – Translate x_2, y_2, z_2 to coordinates centered at O_2 . Since source is at infinity, no change. Solve triangles for azimuth and elevation angles.

sphere are shown in Fig. VI-3. A sidereal day is the interval of time required for Earth to rotate on its axis once with respect to distant stars. One sidereal day is $23^{\text{h}} 56^{\text{m}} 04.09^{\text{s}}$ of mean solar time.

The coordinate transformation for determining azimuth and elevation is straightforward and is best illustrated in Figs. VI-4 through VI-6. An approximation has been made. The radio source has been assumed to be very remote from the center of the earth. If relatively nearby objects such as the moon are to be viewed without significant parallax error, it is necessary to translate the coordinates in Fig. VI-5 outward to the Earth radius at the telescope site before computing the azimuth and elevation angles shown in Fig. VI-6.

3. Angle-Positioning Servo System

A simplified block diagram of the angle-positioning servo systems associated with the radio telescope is shown in Fig. VI-7. The analog servo-drive portion consists of the original NIKE-AJAX system servo amplifiers and motors with angular rate feedback. We have also included the original analog angle-positioning system whose inputs are angles stored in the shaft position of control transformers. This system is not sufficiently accurate to realize 0.01° pointing, but it gives a convenient analog input when

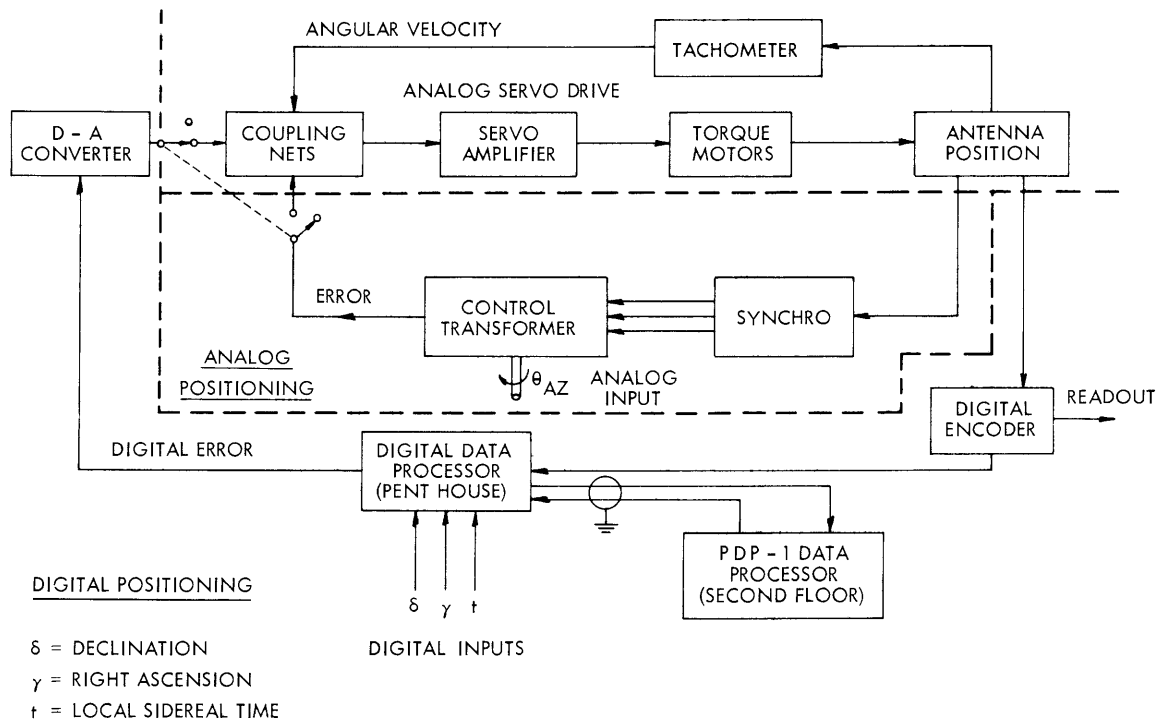


Fig. VI-7. Radio telescope angle-positioning servo systems.

(VI. RADIO ASTRONOMY)

high accuracy is not necessary. There are no provisions for inputs from a coordinate converter. The digital angle-positioning system incorporating digital encoding and the use of a PDP-1 Data Processor for accurate coordinate conversion will be described in this report.

4. Encoding System

An angle encoding system has been build to indicate the actual azimuth and elevation angles. Incremental encoders were used for this purpose. These encoders provide three tracks of level information. Each track is either a logical "one" or "zero." Two

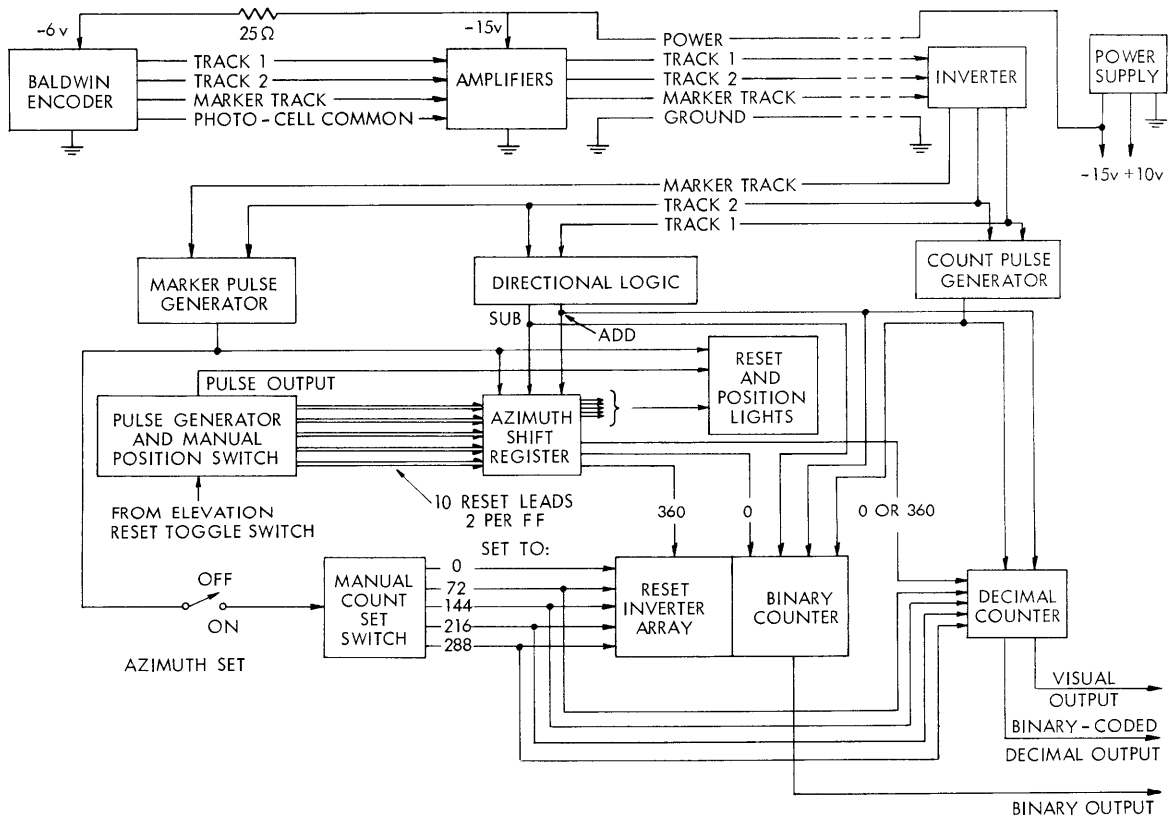


Fig. VI-8. The azimuth-angle encoding system.

of the tracks are fine-data tracks that combine with their logic circuits to produce pulses at every 0.05° rotation of the encoder shaft. From these two tracks direction of rotation is also determined. The third track is a marker that goes to the "one" state once per revolution of the encoder shaft. Position angles are measured by using the marker to set the counter to an initial angle and then counting increments of angle change as

indicated by the two fine-data tracks.

The encoders are mounted on the NIKE-AJAX data axes. These axes are geared to turn 5 revolutions per revolution of the mount axis. This gives increased angular resolution, but introduces angular ambiguity. Five marker pulses now appear per revolution of the mount. A reset system has been designed to permit the operator to indicate one of the 5 possible angle sectors as the correct sector. Because of the five-to-one gearing, the minimum detectable angular increment is 0.01° . A block diagram showing the azimuth encoding system is shown in Fig. VI-8.

5. Digital Data Processor

When the antenna is in the automatic control mode, the system controlling the antenna is the Digital Data Processor (DDP). A block diagram of the DDP is shown in Fig. VI-9. It has decimal input switches in which the operator sets declination and right ascension, the celestial coordinates of a source. The DDP then transmits these inputs and sidereal time from a digital clock to a PDP-1 computer for coordinate transformation once every minute. Computations may also be requested at any time by the operator.

Outputs from the computer consist of three words: azimuth, elevation, and rates. The "rates" output contains information used in updating the azimuth and elevation angles between computations. Each half of the rates word is the number of times the azimuth (or elevation) register is incremented during the next minute. This stepwise incrementing is sufficiently accurate that the angles are always correct within one bit (0.01°) of a linear interpolation.

The azimuth and elevation registers are compared digitally with the mount position angle registers in the encoder system. Differences, which are position errors, are limited, converted to analog signals, amplified, and used as inputs to the error inputs of the antenna analog servo system.

6. PDP-1 Computer

The computer used in conjunction with the DDP is a PDP-1 located on the second floor of the Laboratory, four floors below the DDP. At present, the DDP has control of the PDP-1 at all times when the system is in operation, even though the computer is only utilized for a fraction of a second every minute. Eventually, the PDP-1 time-sharing system will be adapted so that the computer is available to other users when it is not needed by DDP.

Before computation begins, input angles and time are sent to the computer along with their parity — one parity bit per input word. Parity is checked and input repeated if an error is detected. The input is then converted from binary-coded decimal to binary, coordinate conversion is accomplished, and the results sent back to the DDP in binary

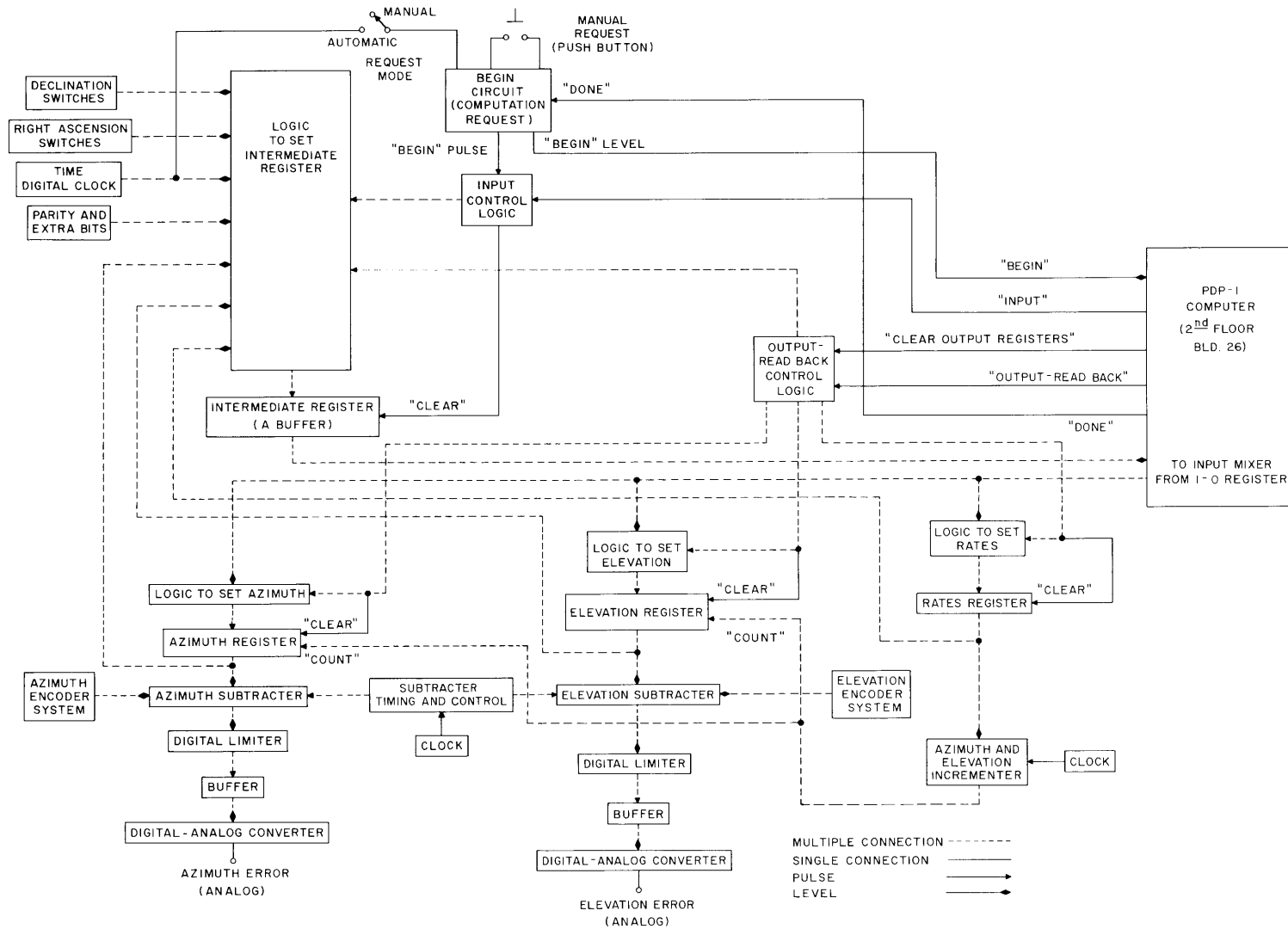


Fig. VI-9. The Digital Data Processor.

form. The DDP stores these results and then sends the stored words back to the computer to be checked bit-for-bit with the computer solution. Output is repeated if an error is detected. When output is successfully completed, a completion pulse is sent to DDP, and the computer returns to the "listen" mode. It then waits for the next request.

An average program takes approximately 7.5 msec to run from request to completion of output. Inaccuracy, which is due to build-up of round-off error, averages $\sim 0.007^\circ$, with a maximum of 0.02° . This error could be eliminated by writing a double-precision program, that is, one that uses two computer words per number.

The present program carries out the coordinate transformation outlined in this report. One of the advantages, however, of a digital computer based system such as this one is its flexibility. Programs may be written to translate coordinates from the center of the earth to its surface to eliminate parallax of nearby objects. Refraction errors resulting from the atmosphere of the earth can be corrected through programming.

J. W. Graham, A. T. Anderson

References

1. Quarterly Progress Report No.66 , Research Laboratory of Electronics, M.I.T., July 15, 1962, pp. 49-52.
2. Quarterly Progress Report No. 70, Research Laboratory of Electronics, M.I.T., July 15, 1963, p. 66.

B. BALLOON OBSERVATIONS OF MICROWAVE EMISSION FROM ATMOSPHERIC OXYGEN

1. Introduction

Microwave propagation in the earth's atmosphere is dominated by the molecular resonances of water vapor and oxygen. Hence these resonances have been studied to determine their effect upon propagation, but very little use has been made of these lines as a tool for determining the physical structure of the atmosphere. The water-vapor line can be detected and studied by ground-based observations because of the low abundance of water vapor. Oxygen, on the other hand, is so abundant that the atmosphere is completely opaque in the center of the resonances. Thus studies of the central lines require the use of high-altitude aircraft or balloons to transport the observing equipment above most of the atmosphere. Ground-based observations can be made of the lines in the far wings of the oxygen complex.¹

The theoretical development of thermal emission from molecular oxygen in the atmosphere indicates that studies of these lines afford a new and competitive means of probing the physical structure of the atmosphere.² Such studies are expected to be

(VI. RADIO ASTRONOMY)

particularly fruitful when performed from an earth-orbiting satellite. The experimental observations in support of the theory are, however, practically nonexistent, and it is desirable to verify the theoretical predictions through balloon flights before a satellite experiment is contemplated. Accordingly, the basic objective of such a program is to provide experimental verification of the theoretical spectrum. Furthermore, the constraints of equipment, such as weight, power, reliability, and so forth, are considerably relaxed for balloon flights as compared with satellite operations; therefore a balloon program affords an ideal means of proving equipment design under operational conditions. A second objective of this program is to design and perfect spectral-line radiometers operating at approximately 5-mm wavelength for spacecraft operation.

2. Design and Construction of Flight Radiometers

During the first year of our program, effort has been directed toward constructing a radiometer suitable for balloon flight. The theoretical part of the program, described in this report, served to define the experiment to be performed and dictated several important equipment parameters. The system that has been designed and built consists of a three-channel radiometer to measure thermal emission from the molecular oxygen line at 61,151 mc and to determine, in a preliminary way, its linewidth, intensity, and dependence on antenna zenith angle. The system is a Dicke superheterodyne radiometer with three IF amplifiers having center frequencies 20 mc, 60 mc, and 200 mc. To avoid duplication of circuitry, the IF amplifiers are time-shared with the low-frequency amplifiers, synchronous detector, and recorder. The system takes advantage of the expected symmetry of the resonance line, so no image rejection is employed. With the local oscillator tuned to 61,151 mc, the radiometer will be responsive to signals in the frequency ranges shown in Table VI-1.

Table VI-1. Passbands of the radiometer.

<u>Channel</u>	<u>Passbands</u>	
1	61,126-61,136 mc	61,166-61,176 mc
2	61,086-61,096	61,206-61,216
3	60,943-60,959	61,343-61,359

This technique was chosen because we wished to avoid the complications that would arise from frequency-scanning the local oscillator across the resonance. In subsequent flights, it may be possible to introduce this feature.

In addition to spectral intensity information, it is important to obtain knowledge of the dependence of intensity with zenith angle. Ideally, this could be obtained by slowly

scanning the antenna from the nadir to the maximum elevation allowable by the constraint of the fully inflated balloon, but this seemed an unnecessary sophistication for the initial flights. An alternative approach, which has been adopted, is to time-share the radiometer between two 6-inch parabolic antennas oriented at zenith angles of 60° and 75° . This should provide preliminary information on the intensity variation with zenith angle and will serve to dictate future experimental requirements.

The radiometer is calibrated by means of a thermal matched load maintained at a preset temperature of approximately 400°K . The temperature of the matched load on the ferrite chopper is also recorded. Thus two reference temperatures are monitored so that both the radiometer sensitivity and base line may be calibrated in temperature units.

The local oscillator was to be a solid-state device utilizing varactor multipliers; however, development on this phase of the program has not progressed sufficiently to meet the flight schedule. Therefore a klystron (Varian VA-250) has been incorporated in the initial flight package. The tube and its power supply is operated in an oil bath and controlled in frequency by a servo-loop from a reference cavity tuned to 61,151 mc.

The time-sharing is controlled by a central clock and programmer with a basic period of approximately 1 minute. A 9-position program is required for three IF channels. The programming is as follows: The 60° zenith-angle antenna is connected to the radiometer for three minutes, during which each IF channel is sampled for 1 minute. This

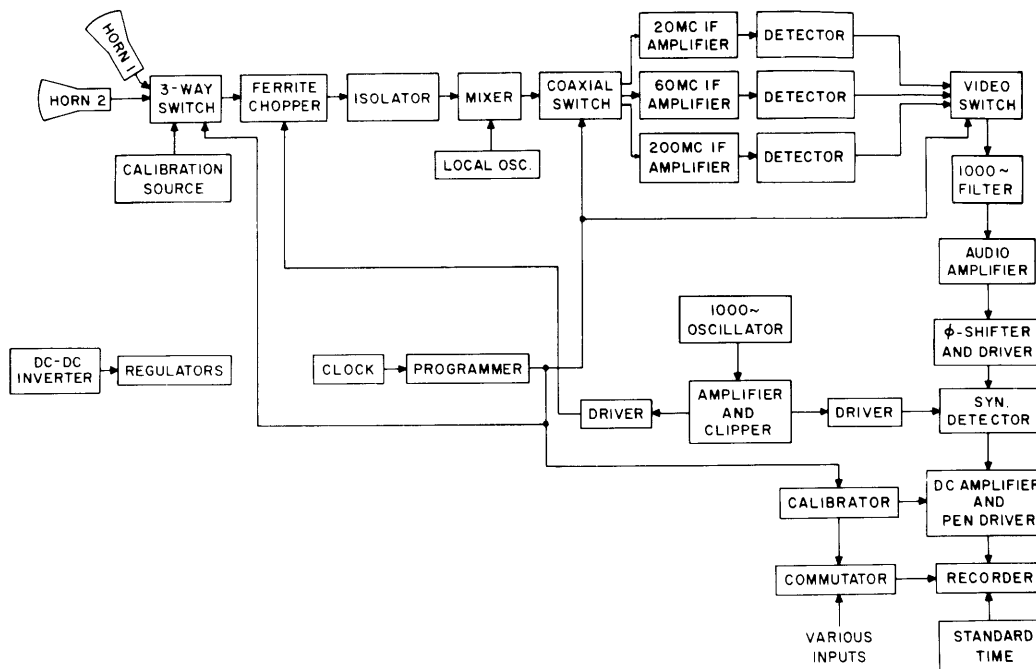


Fig. VI-10. Block diagram of multichannel radiometer.

(VI. RADIO ASTRONOMY)

procedure is then repeated for the 75° zenith-angle antenna and the calibration load. The total cycle is repeated at 9-minute intervals.

Using a balanced crystal mixer, we have measured noise figures of approximately 15 db, 17 db, and 18 db for the 20-mc, 60-mc, and 200-mc channels, respectively. A 10-sec integration time is planned for all channels, which would give rms temperature fluctuations between 2°K and 5°K in the outputs, the amount depending on the channel.

Auxiliary data to be monitored during the flight include various crucial voltages, such as the battery voltage and regulator output, the temperatures of the calibration load, ferrite switch, reference load, battery, front panel, tape recorder, and pressure gauge, the klystron output, the ambient external pressure as determined by an ion gauge, and the outputs of two solar sensors aligned along the antenna beams. These data are fed to the recorder through a commutator.

All data will be recorded in flight on magnetic tape. For this purpose, a special slow-speed recorder has been obtained (Lockheed Electronics Company Model 411F, modified) to allow 8 hours of data storage.

A block diagram of the radiometer is shown in Fig. VI-10, and the flight unit is shown in Fig. VI-11.

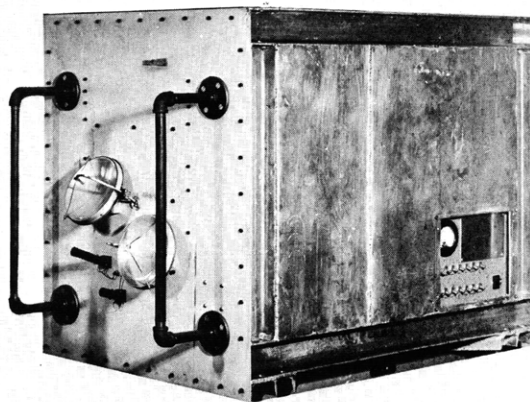


Fig. VI-11. Photograph of equipment packaged for flight.

The total weight of the flight package, including gondola, will be approximately 335 pounds. The radiometer, exclusive of batteries and magnetic tape recorder, weighs 45 pounds; the battery pack, capable of supplying 5 amps for 8 hours at 28 V.D.C., weighs 40 pounds; the magnetic tape recorder and shock-mounted case weighs 50 pounds. The gondola measures 30" × 38" × 27" and weighs approximately 200 pounds.

3. Theoretical Calculations

The microwave properties of molecular oxygen have been rather extensively studied by the techniques of laboratory spectroscopy, and the results obtained thereby form the basis for the theoretical predictions of the spectra of molecular oxygen in the terrestrial atmosphere. Such studies are usually made, however, at low pressures and in pure oxygen – two conditions that are not generally applicable to the earth's atmosphere. Sufficient measurements have been made to enable one to make estimates of the effects of foreign gases, principally nitrogen, and of pressures between 0.1 atm and 1 atm. Therefore it will be possible to make computations of the expected microwave spectra, within the limitations of the uncertainties mentioned.

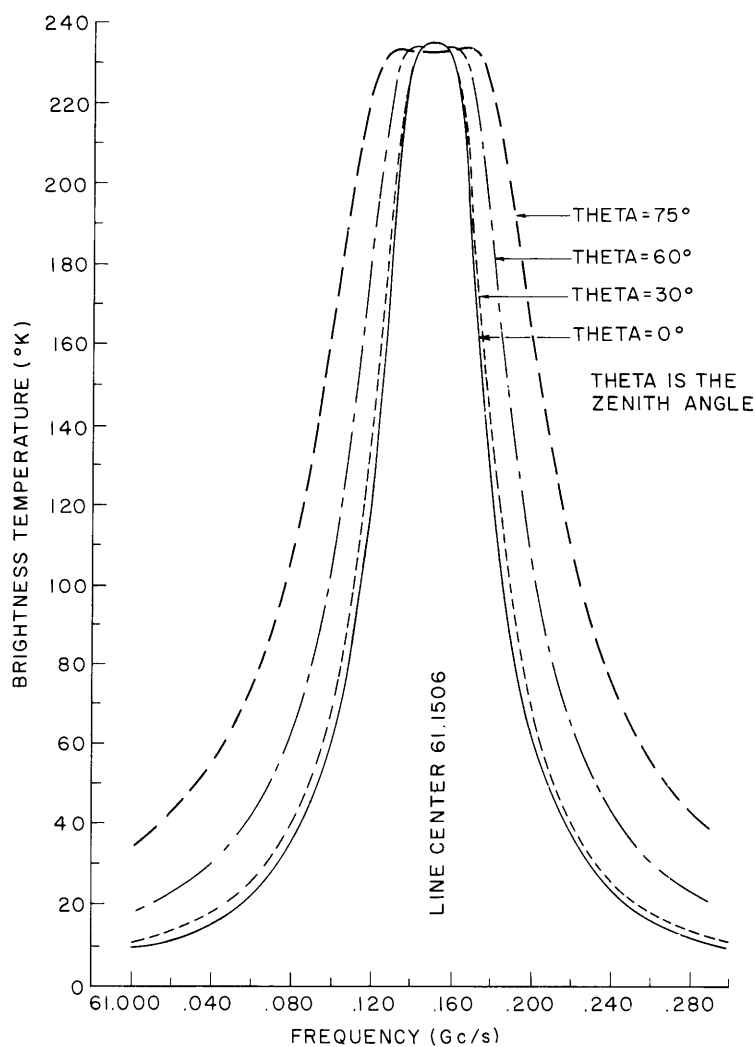


Fig. VI-12. Theoretical spectra of the $N = 9^+$ line at a height of 30 km.

(VI. RADIO ASTRONOMY)

The theoretical spectra of molecular oxygen in the atmosphere can be computed by integrating the equation of transfer with suitable allowances for the variation of temperature, pressure, and chemical composition with altitude. Thus it is necessary to adopt a model for the physical structure of the atmosphere, and the ARDC standard atmosphere has been chosen. The linewidth of the resonance lines will be largely dominated by pressure broadening throughout most of the atmosphere, but there will be a height at which the pressure is so low that other broadening mechanisms can no longer be neglected. For example, the Zeeman splitting of the oxygen lines as a result of the terrestrial magnetic field will be comparable to the pressure broadening at heights of 40-50 km, and Doppler broadening should be included for heights in excess of 50 km. Since these effects are expected to be important for satellite experiments, and our initial balloon flights are not to exceed 30-km altitude, the theoretical spectra computed thus far have included only pressure broadening.

A program for the IBM 7090 computer has been written which calculates the total attenuation and the thermal emission throughout the atmosphere in the frequency range of the molecular oxygen lines. The program is adaptable for any altitude up to 40 km, for any zenith angle between 0° and 180° , and for any desired frequency range and increment. Preliminary computations have been confined to the $N = 9^+$ line at 61,151 mc, since this is the subject of the present experimental program. Figure VI-12 illustrates the results obtained for the oxygen emission at 30 km for various zenith angles. The results of the computations have been used to determine the equipment parameters of the receiver and will be used extensively in the data-interpretation phase of the program after successful flight.

4. Balloon Flight Operations

The equipment was transported to the Balloon Launch Base of the National Center for Atmospheric Research (NCAR), Palestine, Texas, on August 8, 1963 for final pre-flight tests in preparation for a flight. The first flight was attempted at 6:00 a.m. on August 17; a balloon of $3/4$ mil Mylar plastic with a capacity of one million cubic feet of helium was used (see Fig. VI-13). The balloon ruptured almost immediately, as it took the weight of the payload and dropped the radiometer on the runway. But only minor repairs were required, and a second attempt was scheduled for August 19th. This flight was postponed one day because of thunderstorms in the expected recovery area. The second flight, with a slightly lighter payload, and the same type of balloon was attempted at 6:00 a.m. on August 20th, but again the balloon ruptured. A third attempt was made with a reinforced balloon of three million cubic feet capacity, and at 5:23 a.m. on August 22nd the payload was successfully launched. The balloon rose at an average rate of approximately 1000 feet per minute and reached a float altitude of 108,000 feet. During the flight the balloon was followed visually both by airborne and ground recovery teams.

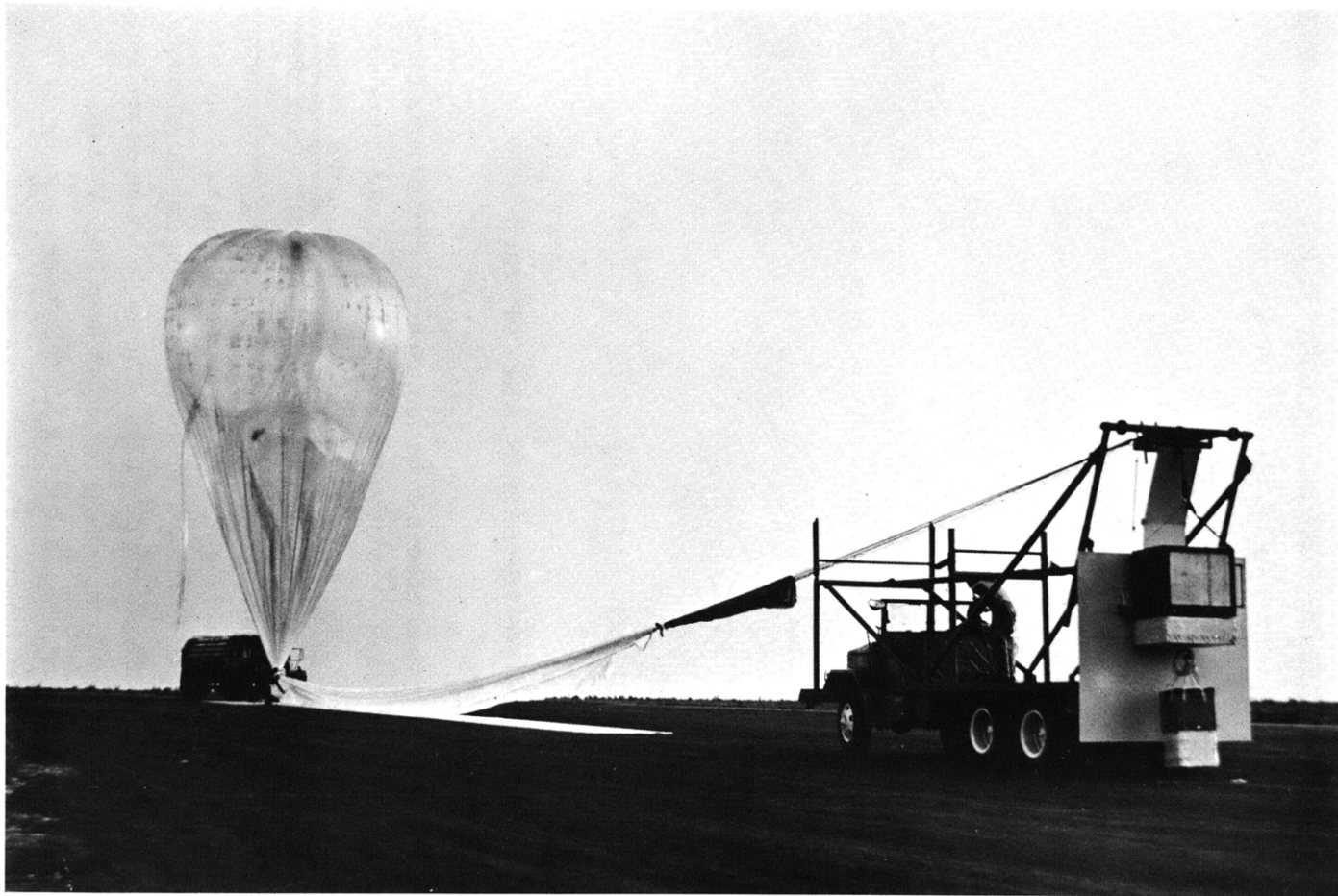


Fig. VI-13. Photograph of radiometer package, launch truck, and balloon just before being released on August 17, 1963.

(VI. RADIO ASTRONOMY)

After slightly more than 6 hours at float altitude the payload was detached from the balloon by radio command and recovered in the open-range country between Water Valley and Robert Lee, Texas, approximately 350 miles west of Palestine. Equipment damage on impact appeared to be less than that sustained during the aborted launches on August 17th and 20th.

5. Flight Performance and Data Analysis

No data analysis has yet been performed at this time. A preliminary playback of the magnetic tape was carried out, however, on the day after the flight at NCAR, Palestine. The equipment operated for approximately 4.5 hours after launch before the klystron apparently became "unlocked" from its stabilizer cavity and ceased oscillation. Before this occurred, the radiometer outputs appeared to saturate the magnetic tape for some of the IF channels. Nevertheless, useful data have been obtained, and a considerable amount of experience has been accumulated which will lead to equipment changes for future flights.

A. H. Barrett, J. C. Blinn III, J. W. Kuiper

References

1. W. Kahan, *Nature* 195, 30 (1962).
2. M. L. Meeks and A. E. Lilley, *J. Geophys. Res.* 68, 1683 (1963).

C. DETECTION OF SCATTERING LAYERS IN THE UPPER ATMOSPHERE (60-140 km)

We report observations of optical echoes from atmospheric constituents (presumably dust) at heights of 60-140 km. They were detected with an optical radar system. The techniques that we used are developments of those that we have reported previously.^{1,2}

The optical radar consists of an RCA designed ruby laser delivering short pulses of approximately 50 nanosec, 0.5 joule at $\lambda = 6940 \text{ \AA}$; a transmitting refracting telescope of 7.5-cm diameter and 201-cm focal length; a receiving reflecting telescope of 32-cm diameter and 270-cm focal length, and of a photometer having an interference filter, 20 \AA wide, and a cooled EMI 9558A photomultiplier. The two telescopes are accurately boresighted and rigidly connected on an equatorial mount (see Fig. VI-14).

All observations reported here were made with the telescopes pointing at the zenith. Each time that the laser was fired the return signals picked up by the photomultiplier were displayed on an oscilloscope and photographed. The return signals originating above 30 km were so weak that it was possible to count individual photoelectrons in each 10-km (66- μ sec) interval up to 180 km. These experiments were carried out during the months of June and July 1963 at Lexington, Massachusetts. They show the Rayleigh molecular

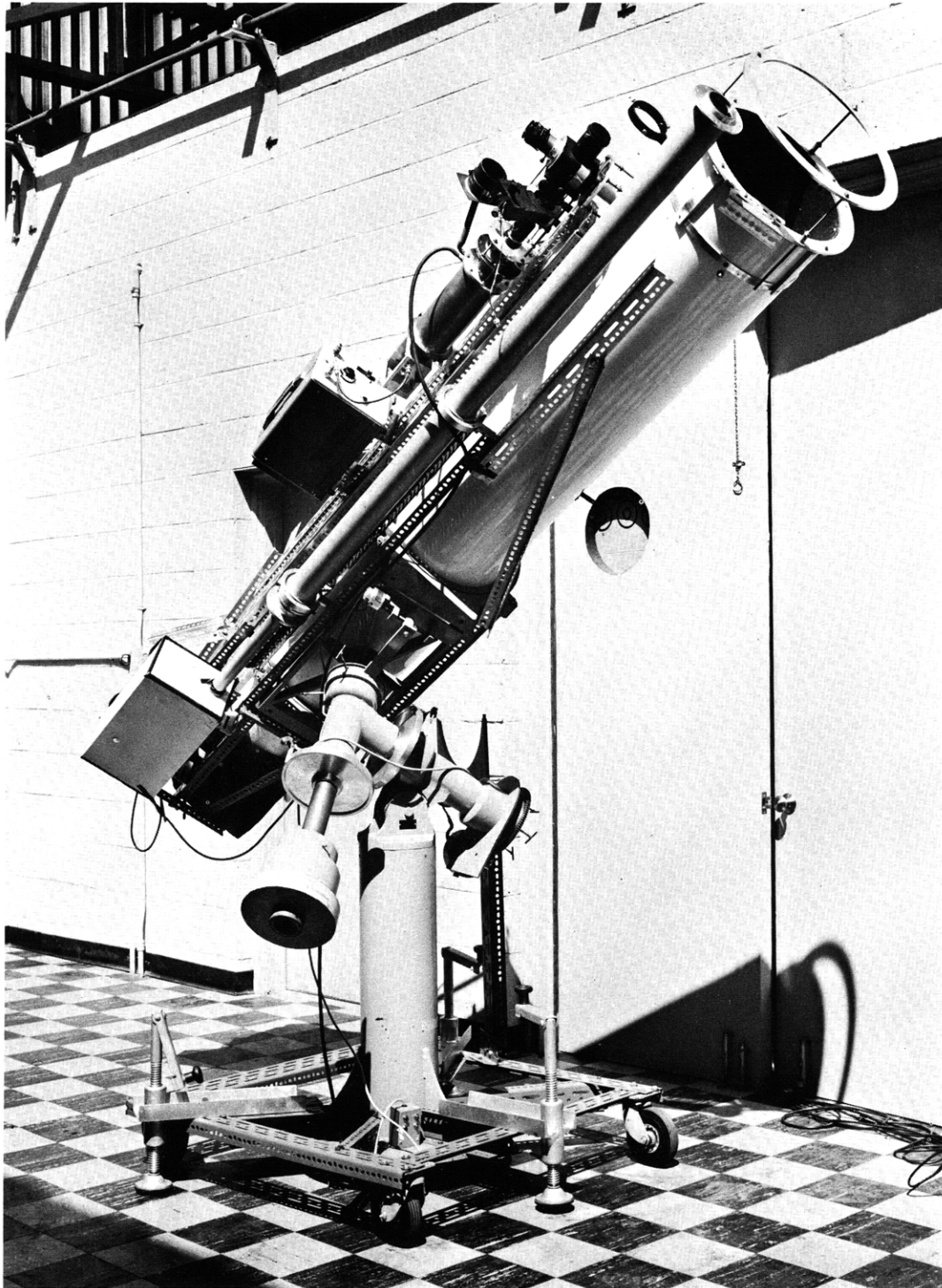


Fig. VI-14. Optical radar system.

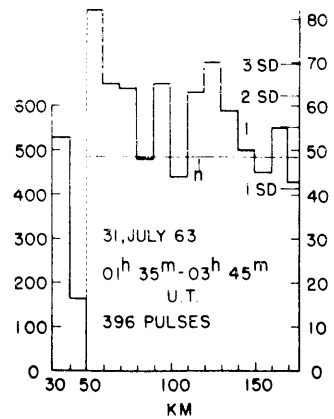
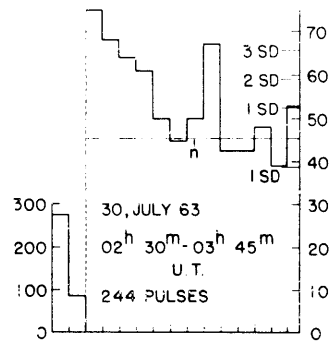
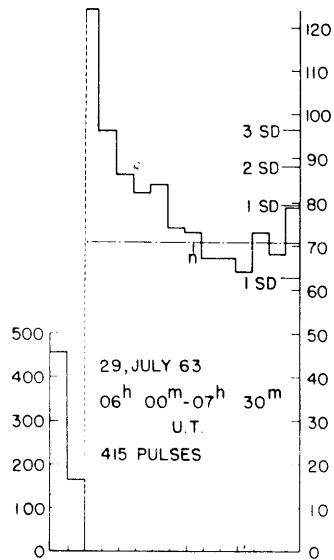
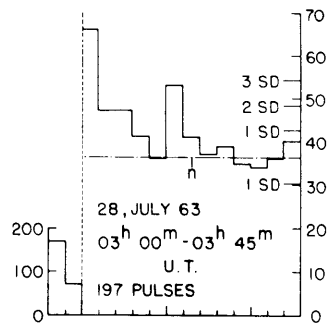


Fig. VI-15. Accumulated photoelectron counts in 10-km range intervals, July 28-31, 1963; n is the average noise level.

(VI. RADIO ASTRONOMY)

scattering at heights up to 50-60 km. At greater heights – up to 140 km – very weak echoes, which we ascribe to dust clouds, were detected. These weak echoes appear to come from two main regions: 60-90 km (often around 80 km), and 110-140 km (often around 120 km).

Figure VI-15 shows the results of the observations on four consecutive days, July 28-31, 1963. This interval covers the period of maximum activity of the δ -Aquarid meteor shower. The sums of the photoelectrons obtained in successive 10-km range intervals are displayed for each night. The noise level, which is represented by photo-multiplier dark current and sky background, is established by taking the average of the returns in the interval 140-180 km. Independent noise measurements taken between laser firings were in substantial agreement with those taken from the extreme ranges. Since the noise has the character of a Poisson process, the standard deviation is taken to be \sqrt{n} , where n is the average noise-level count per range interval. Note that the peaks obtained on 30 and 31 July exceed the average noise level by more than 3 times the standard deviation.

Table VI-2. Occurrence of echoes on nine nights of observation.

U. T.	Range (km)									
	60	70	80	90	100	110	120	130	140	
17 July 1963			x				x	x		
24 July	x									
25 July			x	x						
26 July	x									
27 July							x			
28 July										
29 July										
30 July								x		
31 July								x		

Many similar sets of data showing similar behavior were collected. Table VI-2 was compiled after a preliminary analysis of 9 days of observation. The x's indicate the occurrence of peaks exceeding the average noise level, n , by a factor of $3\sqrt{n}$. The echoes obtained on 31 July are correlated with a backscattering differential cross section per unit volume (averaged between 120 km and

(VI. RADIO ASTRONOMY)

130 km) of approximately $2 \times 10^{-13} \text{ cm}^{-1} \text{ steradians}^{-1}$.

In the absence of independent methods of observation, we cannot say what causes these echoes. One is tempted, however, to compare the lower echoes (~80 km) with the observed heights of noctilucent clouds. We speculate that more distant echoes (~120 km) come from the region of meteoric breakup.

G. Fiocco, L. D. Smullin

References

1. L. D. Smullin and G. Fiocco, *Nature* 194, 1267 (1962); *Proc. IRE* 50, 1703 (1962).
2. G. Fiocco and E. Thompson, *Phys. Rev. Letters* 10, 89 (1963).
3. G. Fiocco, Optical radar to study the earth's atmosphere, *Quarterly Progress Report No. 69*, Research Laboratory of Electronics, M.I.T., April 15, 1963, pp. 28-29.